NRIAG Journal of Astronomy and Geophysics (2013) 2, 266–271

National Research Institute of Astronomy and Geophysics

NRIAG Journal of Astronomy and Geophysics

www.elsevier.com/locate/nrjag

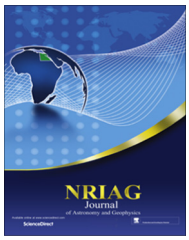

Space base laser torque applied on LEO satellites of various geometries at satellite's closest approach

N.S. Khalifa *

Mathematics Department, Hail University Deanship of Preparatory Year-Girls Branch, Hail, Saudi Arabia
National Research Institute of Astronomy and Geophysics (NRIAG), Cairo, Egypt

Received 20 August 2013; revised 9 December 2013; accepted 11 December 2013
Available online 27 January 2014

KEYWORDS

The Attitude Determination and Control System (ADCS);
Radiation torque;
Solar pumped laser;
Geocentric equatorial coordinate systems;
Spherical and cylindrical coordinate systems and sun synchronous LEO cubesats

Abstract In light of using laser power in space applications, the motivation of this paper is to use a space based solar pumped laser to produce a torque on LEO satellites of various shapes. It is assumed that there is a space station that fires laser beam toward the satellite so the beam spreading due to diffraction is considered to be the dominant effect on the laser beam propagation. The laser torque is calculated at the point of closest approach between the space station and some sun synchronous low Earth orbit cubesats. The numerical application shows that space based laser torque has a significant contribution on the LEO cubesats. It has a maximum value in the order of 10^{-8} Nm which is comparable with the residual magnetic moment. However, it has a minimum value in the order 10^{-11} Nm which is comparable with the aerodynamic and gravity gradient torque. Consequently, space based laser torque can be used as an active attitude control system.

1. Introduction

The Attitude Determination and Control System (ADCS) is to stabilize the spacecraft against attitude disturbing influences resulting from the environment. Satellite active attitude control can be achieved by number of different actuators: reaction wheels, thrusters, control moment gyroscopes or magnetic torquers. However, the magnetic torquer is widely used actuators for geostationary satellites, small satellites, and microsatellites. These high-tech devices interact with the Earth's magnetic field and create control torque, which can be adjusted to the required value. Combined with one or more reaction wheels, they provide all control you need to maintain your spacecraft's attitude (Karla, 2009; Vincent, 2010).

Unlike thrusters, magnetorquers are lightweight, reliable, and energy-efficient. A further advantage over momentum wheels and control moment gyroscopes is the absence of moving parts and therefore significantly higher reliability. However, they require a thoughtful design and careful assembly.

The main disadvantage of magnetorquers is that the strength of the magnets should be chosen to be strong enough to overcome the greatest expected disturbances (as given in Table 1). A broader disadvantage is the dependence on Earth's

* Address: National Research Institute of Astronomy and Geophysics (NRIAG), Cairo, Egypt. Tel.: +966 551163874.
E-mail address: asmaa_2000_2000@yahoo.com.
Peer review under responsibility of National Research Institute of Astronomy and Geophysics.

Production and hosting by Elsevier

2090-9977 © 2014 Production and hosting by Elsevier B.V. on behalf of National Research Institute of Astronomy and Geophysics.
http://dx.doi.org/10.1016/j.nrjag.2013.12.004

Table 1 Worst-case expected disturbance torques for a 1-U CubeSat at 700 km (Samir, 2009).

The source	Torque (Nm)
Aerodynamics	8.7×10^{-10}
Gravity gradient	6.8×10^{-10}
Solar pressure	3.8×10^{-9}
Residual Magnetic Moment	4.5×10^{-7}
Total	4.6×10^{-7}

magnetic field strength, making this approach unsuitable for deep space missions, and also more suitable for low Earth orbits as opposed to higher ones like the geosynchronous. The dependence on the highly variable intensity of Earth's magnetic field is also problematic because the attitude control problem becomes highly nonlinear. It is also impossible to control attitude in all three axes even if the full three coils are used, since the torque can be generated only perpendicular to the Earth's magnetic field vector (Samir, 2009; Vincent, 2010).

Recently, the possibility of using laser power for space applications becomes of great interest. There are several advantages of lasers over other techniques of beamed power; the laser receiver is the solar array, so no new receiver technology is needed. Moreover, space laser beam suffers a less amount of atmospheric attenuation also it is safe in use where it cannot produce damage in the satellite surface (El-saftawy et al., 2007; El-saftawy and Makram, 2004; Geoffrey, 1994; Khalifa, 2009).

Compared with electrically powered lasers, solar laser is much simpler and more reliable due to the complete elimination of the electrical power generation and conditioning equipments. Many authors studied the feasibility of concentrating and splitting of solar radiation in satellites for laser pumping by either direct or indirect conversion methods (Yogev et al., 1996; Geoffrey, 1994; Almeida et al., 2012).

Several researchers have investigated the solar pumped Nd:YAG and Nd:Cr lasers have been demonstrated with power levels up to 25 W, and iodine lasers at up to 10 W. Most lasers, such as the Nd:YAG discussed above, absorb light only in selected bands. This leads to an inefficient absorption of the broad-band solar spectrum. A semiconductor, on the other hand, absorbs all photons with energy greater than the band gap. Thus, solar pumped semiconductor lasers could have considerably higher efficiencies than other solar pumped lasers. So, solar pumped semiconductor lasers are thus an excellent candidate for space-based energy transmission (Geoffrey, 1994).

With the intention of overcoming some disadvantages of the traditional attitude actuators, the issue of this work is to investigate the feasibility of using a space solar pumped laser to produce a torque. Assuming that there is a space station that fires laser beam toward some low Earth orbit satellites, the torque is calculated at the point of their closest approach.

2. Laser torque model

2.1. Laser intensity

At far distance of the celestial bodies, the atmosphere is rarefied (i.e. the particle density is very low). So, beam spread due to diffraction is considered to be the dominant effect on the laser beam propagation. Then the beam intensity is given by El-saftawy et al. (2007) and Khalifa (2009):

$$S=\frac{P}{\pi D^2\theta^2} \tag{1}$$

where, P is the laser power, θ is the laser divergence and D is the propagation distance.

2.2. The laser force

The total radiant force exerted on a flat non-perfectly reflecting surface is given by Mc Innes Colin (1999):

$$\bar{f}=\frac{SA}{C}\psi\hat{m} \tag{2}$$

where,

$$\psi=\left[4\rho'\beta\cos^4\eta+2(1+\rho'\beta)\left(B_f\rho'(1-\beta)+\alpha'\frac{\varepsilon_f B_f-\varepsilon_b B_b}{\varepsilon_f+\varepsilon_b}\right)\cos^3\eta+\left\{\left(B_f\rho'(1-\beta)+\alpha'\frac{\varepsilon_f B_f-\varepsilon_b B_b}{\varepsilon_f+\varepsilon_b}\right)^2+(1-\rho'\beta)^2\right\}\cos^2\eta\right]^{1/2} \tag{3}$$

where A is the projected area, $\hat{m}$ is a unit vector directed through the force direction, C is the speed of light and S is the radiation irradiance, η is the incident angle, β is the satellite surface specularity, ρ' is the satellite surface reflectivity, B_f and B_b are the non-Lambartian coefficient of the front and back surfaces of the spacecraft, respectively, α' is the spacecraft absorption coefficient, ε_f and ε_b are the front and back surface emissivity, respectively.

In our case we will consider a solar-pumped laser station, Sat1, fires laser toward another satellite, Sat2, at the point of their closest approach. For non-perfectly reflecting surfaces, the force vector, $\hat{m}$, is not directed normal to the surface. But, it inclines by an angle ϑ to the incident direction, D, as depicted in Fig. 1. Considering the effect of the surrounding medium on the beam propagation, the force components in the incident direction will be:

$$\begin{aligned}\bar{f}_D&=\tfrac{SA}{C}\psi\cos\vartheta\,\widehat{D}\\&=\tfrac{P_o A\psi}{\pi D^2\theta^2}\cos\vartheta\overline{D}\end{aligned} \tag{4}$$

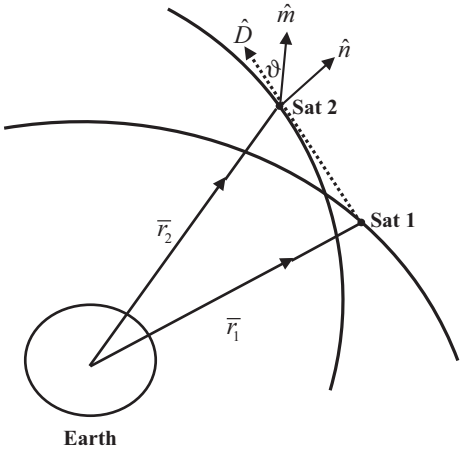

Figure 1 The laser intensity delivered from Sat1 to Sat 2.

2.3. The coordinate systems

The geocentric equatorial system with unit the vectors; $\hat{e}_x$ directed parallel to the Earth equatorial plane, $\hat{e}_y$ directed in the plane that contains the meridian of the sub-satellite point and $\hat{e}_z$ directed normal to the equatorial plane is used. As shown in Fig. 1, the incident radiation vector, $\overline{D}$, is given by:

$$\overline{D} = \bar{r}_2 - \bar{r}_1, \tag{5}$$

where $\bar{r}_i$ is the satellite position vector which is given by Escobal (1965):

$$\bar{r}_i(E_i) = a_i(cosE_i - e_i)\overline{P}_i + b_i sinE_i\overline{Q}_i \tag{6}$$

where E_i ($i = 1, 2$) are the eccentric anomalies, a_i are the semi-major axes and $b_i = a_i\sqrt{1-e_i^2}$ are the semi-minor axes. The unit vectors of the perifocal coordinate system of the two orbits $\overline{P}_i$, $\overline{Q}_i$ are given by Escobal (1965):

$$\overline{P}_i = \begin{pmatrix} \cos\omega_i\cos\Omega_i - \sin\omega_i\sin\Omega_i\cos i_i \\ \cos\omega_i\sin\Omega_i + \sin\omega_i\cos\Omega_i\cos i_i \\ \sin\omega_i\sin i_i \end{pmatrix} \tag{7}$$

$$\overline{Q}_i = \begin{pmatrix} -\sin\omega_i\cos\Omega_i - \cos\omega_i\sin\Omega_i\cos i_i \\ -\sin\omega_i\sin\Omega_i + \cos\omega_i\cos\Omega_i\cos i_i \\ \cos\omega_i\sin i_i \end{pmatrix} \tag{8}$$

Substitute Eqs. (6)–(8) into Eq. (5). The separating distance vector is given by:

$$\overline{D} = D_x\hat{e}_x + D_y\hat{e}_y + D_z\hat{e}_z \tag{9}$$

where

$$\begin{aligned} D_x = {} & a_2(cosE_2 - e_2)(\cos\omega_2\cos\Omega_2 - \sin\omega_2\sin\Omega_2\cos i_2) \\ & - a_1(cosE_1 - e_1)(\cos\omega_1\cos\Omega_1 - \sin\omega_1\sin\Omega_1\cos i_1) \\ & - b_2 sinE_2(\sin\omega_2\cos\Omega_2 + \cos\omega_2\sin\Omega_2\cos i_2) \\ & + b_1 sinE_1(\sin\omega_1\cos\Omega_1 + \cos\omega_1\sin\Omega_1\cos i_1) \end{aligned} \tag{10}$$

$$\begin{aligned} D_y = {} & a_2(cosE_2 - e_2)(\cos\omega_2\sin\Omega_2 + \sin\omega_2\cos\Omega_2\cos i_2) \\ & - a_1(cosE_1 - e_1)(\cos\omega_1\sin\Omega_1 + \sin\omega_1\cos\Omega_1\cos i_1) \\ & - b_2 sinE_2(\sin\omega_2\sin\Omega_2 - \cos\omega_2\cos\Omega_2\cos i_2) \\ & + b_1 sinE_1(\sin\omega_1\sin\Omega_1 - \cos\omega_1\cos\Omega_1\cos i_1) \end{aligned} \tag{11}$$

$$\begin{aligned} D_z = {} & a_2(cosE_2 - e_2)\sin\omega_2\sin i_2 - a_1(cosE_1 - e_1)\sin\omega_1\sin i_1 \\ & + b_2 sinE_2\cos\omega_2\sin i_2 \\ & - b_1 sinE_1\cos\omega_1\sin i_1 \end{aligned} \tag{12}$$

2.4. Satellites' closest approach

The separating distance between the two satellites is given by:

$$\begin{aligned} D = |\overline{D}| = {} & \sqrt{(\bar{r}_2 - \bar{r}_1)(\bar{r}_2 - \bar{r}_1)} = [(a_2(\cos E_2 - e_2))^2 \\ & + (b_2\sin E_2)^2 + (a_1(\cos E_1 - e_1))^2 + (b_1\sin E_1)^2 \\ & - 2a_1a_2(\cos E_1 - e_1)(\cos E_2 - e_2)(\overline{P}_1.\overline{P}_2) \\ & - 2a_2b_1\sin E_1(\cos E_2 - e_2) \times (\overline{P}_2.\overline{Q}_1) \\ & - 2a_1b_2\sin E_2(\cos E_1 - e_1)(\overline{P}_1.\overline{Q}_2) \\ & - 2b_2b_1\sin E_1\sin E_2(\overline{Q}_2.\overline{Q}_1)]^{\frac{1}{2}} \end{aligned} \tag{13}$$

The problem of close approach can be formulated as follows Dybczynski et al. (1986):

$$\underset{(E_1,E_2)\in U}{\forall} D(E_1, E_2) \geqslant 0, \tag{14}$$

there obviously exists such a value D^* that:

$$D^* = \inf\{D(E_1, E_2)|(E_1, E_2) \in U\}, \tag{15}$$

where U is the domain of the function D. Every pair $(E_1, E_2) \in U$ satisfying $D(E_1^*, E_2^*) = D^*$ are solutions to our problem. According to Weierstrass theorem, if U is a compact set and D is a continuous function over U then D has at least one minimum value somewhere in U. If U^* is the subset of all pairs (E_1^*, E_2^*), then $D^*(E_1^*, E_2^*) \in U$ which is nonempty, if we restrict conditions on D. The necessary and sufficient conditions of the local minimum existence are:

$$D_1' = \frac{\partial D(E_1, E_2)}{\partial E_1} = 0, \tag{16}$$

and

$$D_2' = \frac{\partial D(E_1, E_2)}{\partial E_2} = 0. \tag{17}$$

where the roots of Eqs. (16) and (17) must verify the following conditions:

$$D_1''(E_1, E_2) = \frac{\partial^2 D(E_1, E_2)}{\partial E_1^2} > 0, \tag{18}$$

$$D_2''(E_1, E_2) = \frac{\partial^2 D(E_1, E_2)}{\partial E_2^2} > 0, \tag{19}$$

and

$$D_1''D_2'' - (D_{12}'')^2 > 0 \tag{20}$$

where $D_{12}'' = \frac{\partial^2 D(E_1,E_2)}{\partial E_1 \partial E_2}$.

In this work the proposed method tries to find a numerical solution of the problem of close approach determination. It is based on performing a successive scanning over the two variables E_1 and E_2, for one revolution, to find an initial guess ensures convergence to the local minimum. Where, this pair of (E_1, E_2) must verify the conditions of the existence of local minimum at that point, given by Eqs. (18)–(20). Then use this pair to start the iterations using the generalized method of Newton – Raphson to locate the closest approach (Khalifa et al., 2008; Khalifa, 2009).

Computational algorithm

- Purpose: to pick an appropriate guess of E_1 and E_2 associated with the smallest separating distance, using Eqs. (6)–(13), by successive scanning over the two orbits for one revolution. Then locate the point of closest approach, at that revolution, numerically using the generalized form of Newton Raphson method.
- Computational sequence:
  1. Set $E_2^o = 0.0^o$.
  2. Change E_1 from 0.0^o to 360^o with step size of 1^o .
  3. Calculate $r_2(E_2^o) = r_2(0.0^o)$ and $r_1(0.0^o)$, $r_1(0.1^o)$, $r_1(0.2^o)$, …, $r_1(360^o)$using Eqs. (6)–(8).
  4. Calculate $D(0.0^o, 0.0^o)$, $D(1^o, 0.0^o)$, …, and $D(360^o, 0.0^o)$ using Eqs. (9)–(13).
  5. Set $E_2^o = 1^o$.
  6. Repeat steps 2–4.
  7. Repeat steps from 1 to 4 by changing E_2^o from 2^o to 360^o with step size of 1^o.

8. Select the pair (E_1^1, E_2^1) associated with the smallest separating distance $D(E_1^1, E_2^1)$.
9. Repeat steps 1–7 on the neighborhood of the pair (E_1^1, E_2^1) with step size of 0.1^o and then select the pair (E_1^2, E_2^2) associated with the smallest separating distance $D(E_1^2, E_2^2)$.
10. Repeat steps 1–7 on the neighborhood of new pair (E_1^2, E_2^2) results from step 9 with step size of $.01^o$ and so on with step size of $.001^o$, $.0001^o$, ..., ect to reach the closest approach with the required accuracy.
11. Start Newton Raphson iteration by substituting the initial values $E_{1(0)}$ and $E_{2(0)}$ which were obtained by step 10.
12. Terminate the iteration at the required accuracy.
13. Calculate $D(E_1, E_2)$ with E_1 and E_2 obtained by step 12.
14. Verifying that $D(E_1, E_2)$ is the minimum distance by applying the conditions of local minimum given by Eqs. (18)–(20).
15. The algorithm is completed.

2.5. The laser torque

The radiation torque, $\widehat{N}$, acting on a spacecraft is given by the general expression (Beletskii, 1966; Harris and Lyle, 1969; Wertz, 1978; Zanardi and Moraes, 1999):

$$\overline{N} = \int \overline{R} \times d\overline{f}, \tag{21}$$

where $\overline{R}$ is the vector from the spacecraft's center of mass to the element of satellite projected area dA. The geocentric components of laser torque, $\widehat{N}$, acting on a spacecraft are given by:

$$N_x = \frac{P_o}{\pi c D^3 \theta^2} \psi \cos\vartheta \int (R_y D_z - R_z D_y) dA \tag{22}$$

$$N_y = \frac{P_o}{\pi c D^3 \theta^2} \psi \cos\vartheta \int (R_z D_x - R_x D_z) dA \tag{23}$$

$$N_Z = \frac{P_o}{\pi c D^3 \theta^2} \psi \cos\vartheta \int (R_x D_y - R_y D_x) dA \tag{24}$$

For high laser repetition rate, many laser shots fire toward the satellite over an interval of time each one of intensity S. Consequently, the laser force can be considered as a continuous function, so, the total laser torque over an interval of time, $I = t_1 - t_o$, is given by:

$$\overline{N}_I = \int_{t=t_o}^{t=t_1} \overline{N} dt, \tag{25}$$

where t_o is the time of the starting laser firing and t_1 is the time of its stop.

In order to evaluate the previous integrals, the vector $\overline{R}$ must be determined. So, satellite geometry must be considered. In the next sections, three particular cases; circular cylindrical satellite, spherical satellite and satellite of complex shape will be studied.

2.6. Application of laser torque

2.6.1. Laser torque on circular cylindrical satellite

The position vector of the surface elements can be expressed in terms of a coordinate system with its origin lying in the geometric center of the satellite and the vectors $\hat{e}_{x'}, \hat{e}_{y'}$ and $\hat{e}_{z'}$ as follows:

$$\overline{R}_c = \rho\cos\phi\hat{e}_{x'} + \rho\sin\phi\hat{e}_{y'} + z\hat{e}_{z'} \tag{26}$$

where ρ is the radius of the circular base and ϕ is the azimuthal angle. The position vector, $\overline{R}_c$, can be transformed into geocentric coordinate as follows:

$$\overline{R}_c = R_{cx}\hat{e}_x + R_{cy}\hat{e}_y + R_{cz}\hat{e}_z \tag{27}$$

with

$$R_{cx} = \rho\cos\phi + r(\cos\Omega\cos(\omega+\upsilon) - \sin\Omega\sin(\omega+\upsilon) \times \cos i) \tag{28}$$

$$R_{cy} = \rho\sin\phi + r(\sin\Omega\cos(\omega+\upsilon) + \cos\Omega\sin(\omega+\upsilon)\cos i) \tag{29}$$

$$R_{cz} = z + r\sin(\omega+\upsilon)\sin i \tag{30}$$

The illuminated surfaces of the cylinder satellite are a circular flat surface of radius ρ and an area $A_1 = \pi\rho^2$ in addition to a portion σ of the cylinder side of height H with an area, $A_2 = 2\sigma\pi\rho H$, as in Fig. 2.

Substituting into Eqs. (28)–(30) and integrating over the areas A_1 and A_2, laser torque applied on a cylindrical satellite is obtained.

2.6.2. Laser torque on spherical satellite

The position vector of the surface elements can be expressed in terms of a coordinate system with its origin lying in the geometric center of the satellite and the vectors $\hat{e}_{x'}, \hat{e}_{y'}$ and $\hat{e}_{z'}$ as follows:

$$\widehat{R}_s = \rho\cos\vartheta\sin\phi\hat{e}_{x'} + \rho\sin\phi\sin\vartheta\hat{e}_{y'} + \rho\cos\phi\hat{e}_{z'} \tag{31}$$

where ρ is the radius of the sphere, ϑ is the polar angle and ϕ is the azimuthal angle. The position vector, $\widehat{R}_s$, can be transformed into geocentric coordinate as follows:

$$\overline{R}_s = R_{sx}\hat{e}_x + R_{sy}\hat{e}_y + R_{sz}\hat{e}_z \tag{32}$$

with

$$R_{sx} = \rho\cos\vartheta\sin\phi + r(\cos\Omega\cos(\omega+\upsilon) - \sin\Omega\sin(\omega+\upsilon)\cos i) \tag{33}$$

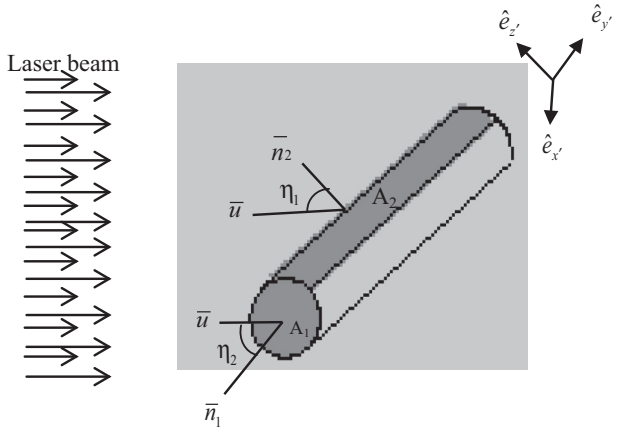

Figure 2 The illuminated surfaces of the circular cylindrical satellite.

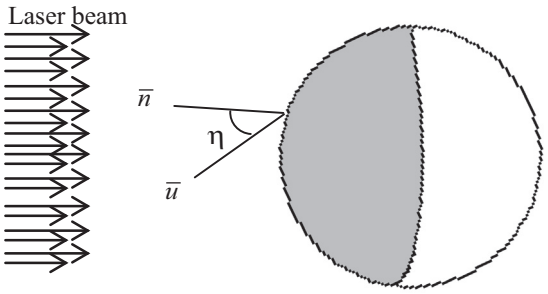

Figure 3 The illuminated surfaces of the spherical satellite.

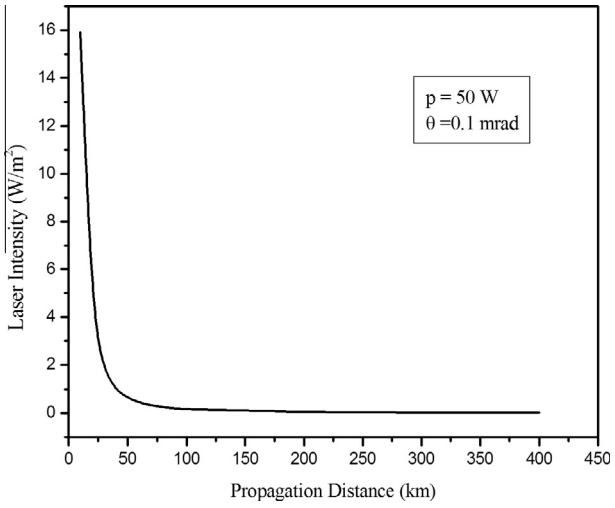

Figure 4 Laser beam propagation outside the Earth's atmosphere for different distance of propagation.

$$R_{sy} = \rho \sin\phi \sin\vartheta + r(\sin\Omega\cos(\omega+\upsilon) + \cos\Omega\sin(\omega + \upsilon)\cos i) \quad (34)$$

$$R_{sz} = \rho\cos\phi + r\sin(\omega+\upsilon)\sin i \quad (35)$$

The illuminated surfaces of the spherical satellite can be considered as a hemisphere with an area $A = 2\pi\rho^2$, as shown in Fig. 3.

Substituting into Eqs. (33)–(35) and integrating over the area A, the laser torque applied on a spherical satellite is obtained.

2.6.3. Laser Torque on Satellite of complex shape

Radiation torque depends basically on the satellite geometry. For satellites of complex shape, torque calculation is very complicated. The usual procedure is to split the satellite surface into number of surfaces. Then radiation torque is approximated using the following scheme Harris and Lyle (1969):

1. Approximate each surface by means of simple geometric shapes (planes, cylinders, cones, spheres, ..., etc.).
2. Determine the torque applied on each surface independently using the above mentioned equations in case of spherical and cylindrical surfaces.
3. The total torque applied over the whole spacecraft is obtained by vector sum of all torques applied on each elementary surface.

However, the above procedure has many difficulties to be applied. Various factors affecting the computed torque e.g. changes in the optical characteristics of each surface, bending of a boom, rotation of solar panel, ..., etc. cannot be considered. Consequently, the computed values are not precisely determining the radiation torque on a spacecraft Harris and Lyle (1969).

3. Numerical application

Assuming that the solar pumped laser station fires laser beam of 50 KW power and 0.1 mrad divergence, the laser beam propagation outside the Earth's atmosphere is illustrated in the following figure:

As shown in Fig. 4, the laser intensity has a significant dependency on the propagating distance. It has a maximum value ~16 W/m^2 for propagating distance of about 10 km. However, it has a minimum value ~.009 W/m^2 for propagating distance of about 400 km.

Table 2 Orbital elements of the solar pumped laser station.

Semi-major axis (km)	Mean motion	Argument of perigee	Longitude of ascending node	Eccentricity	Mean anomaly	Inclination
6997.26	12.44	328.83°	6.46	.0145	31.2°	14.8 °

Table 3 Space based laser torque affecting on some sun synchronous LEO cubesats.

Satellite	NORD ID	Semi-major axis (km)	D (km)	Torque (Nm)
CUTE 1.7 APD II (1U)	32785	6996.95	11.1	6.5×10^{-9}
COMPASS I (1U)	32787	6993.03	110.9	1.8×10^{-9}
SEED (1U)	32791	6995.19	119.1	1.4×10^{-9}
AAUSAT CUBESAT II (1U)	32788	6991.85	238.5	7.6×10^{-11}
DELFI C3 (3U)	32789	6985.87	482.3	6.7×10^{-9}

Assuming that there is a space station carries a solar-pumped laser system lie in LEO and at a given time it has the following orbital elements: Table 2)

In the present work, the laser torque is calculated under the following postulates:

1. The radiation falls normal to the satellite surface (i.e. $\eta = 0$).
2. The satellite projected area is half of its total area.
3. The cubesat's thermo-optical properties are constrained to CalPoly's specifications (2012).

Based on the previous postulates and applying the algorithm of closest approach at a given time, the laser torque is calculated for some sun synchronous LEO cubesats and illustrated in the following table:

As illustrated in Table 3, the laser torque has a maximum value in the order of 10^{-8} which is comparable with the residual magnetic moment (given in Table 1). However, it has a minimum value in the order of 10^{-11} which is comparable with the aerodynamic and gravity gradient torque (given in Table 1).

4. Conclusion

A new application of utilizing laser power in space is presented. A simple model of radiation torque affecting on satellites of various shapes is formulated. The model is based on the use of space based laser which suffers minimum beam attenuation due to its propagation outside the Earth's atmosphere. The current numerical test confirms that the laser torque has a significant contribution on the low Earth orbit satellites. The laser torque has a maximum value in the order of 10^{-8} which is comparable with the residual magnetic moment. However, it has a minimum value in the order of 10^{-11} which is comparable with the aerodynamic and gravity gradient torque. So, we can conclude that the laser torque can be used as a new active attitude control system.

References

Almeida, J., Liang, D., Guillot, E., 2012. Improvement in solar-pumped Nd:YAG laser beam brightness. Opt. Laser Technol. 44 (7), 2115–2119.

Beletskii, V.V., 1966. Motion of an artificial satellite about its center of mass, NASA translation, NASA TF – 429.

Cal Poly SLO, CubeSat design specification, (2012). Available from: <http://www.cubesat.org/images/developers/cds_rev12.pdf>.

Dybczynski, P.A., Jopek, T.J., Serafin, R.A., 1986. On the minimum distance between two Keplerian orbits with a common focus. Celestial Mechanics 38.

El-Saftawy, M.I., Afaf, M., Abd El-Hameed, Khalifa, N.S., 2007. Analytical studies of laser beam propagation through the atmosphere. In: Proceeding of 6th International Conference on Laser Science and Applications (ICLAS-07), Cairo, Egypt.

El-saftawy, M.I., Makram, Ibrahim, 2004. The laser shots as a perturbing force on spacecraft's orbit. NRIAG. J. Astro. Astro. Phys. (special issue).

Escobal, P.R., 1965. Methods of Orbit Determination. John Wiley and Sons Inc., New York, London, Sydney.

Geoffrey A. Landis, 1994. Prospects for solar pumped semiconductor lasers. In: SPIE Proceedings, vol. 2121.

Harris, M., Lyle, R., 1969. Spacecraft radiation torque, NASA space vehicle design criteria (guidance and control) NASA SP-8027.

Karla Patricia Vega, 2009. Attitude Control System for CubeSat for Ions, Neutrals, Electrons and MAGnetic Field (CINEMA) (MSc. thesis). University of California, Berkeley.

Khalifa N.S., El-Saftawy, M.I., Khalil, Kh I., Abd El-Salam, F.A., Ahmed, M.K.M., 2008. Space based laser perturbation at satellites' closest approach. In: First Middle East and Africa IAU-Regional Meeting Proceedings MEARIM No. 1.

Khalifa N.S., 2009. Effect of an Artificial Radiant Force on the Spacecraft's Orbit, (Ph.D. thesis). Cairo University.

Mc Innes Colin, R., 1999. Solar Sailing: Technology, Dynamics and Mission Applications, Springer-Praxis Series in Space, Science and Technology.

Samir Rawashdeh, 2009. Passive Attitude stabilization for small satellites (Msc thesis). University of Kentucky, Kentucky.

Vincent Francois-Lavet, 2010. Study of Passive and Active Attitude Control Systems for the OUFTI Nanosatellites (Msc. thesis). University of Liège.

Wertz, J.R. (Ed.), 1978. Spacecraft Attitude Determination and Control. D. Reidel Dordrecht, Holland.

Yogev, A., Appelbaum, J., Oron, M., Yehezkel, N., 1996. Concentrating and splitting of solar radiation for laser pumping and photovoltaic conversion. J. Propul. Power 12 (2).

Zanardi, M.C., Moraes, Vilhena de, 1999. Analytical and semi-analytical analysis of an artificial satellite's rotational motion. Celest. Mech. Dyn. Astron. 75.